Journal of Metallurgy and Materials Science, Vol. 62, No. 3-4,July-December2020, pp. 41-48
Printed in India, © NML, ISSN 0972-4257

Limiting platelet adhesion in stainless steel bio-implants through microstructural modification

G. PERUMAL[1], A. CHAKRABARTI[2], S. PATI[2], S. SINGH[3], V. REDDY[4], H.S. GREWAL[1], G. MANIVASAGAM[4] and H. S. ARORA[1],*

[1]Surface Science and Tribology Laboratory, School of Mechanical Engineering, Shiv Nadar University, Uttar Pradesh 201314, India

[2]Department of Life Sciences, School of Natural Sciences, Shiv Nadar University, Uttar Pradesh 201314, India

[3]Special Center for Molecular Medicine, Jawaharlal Nehru University, New Delhi 110067, India

[4]Centre for BioMaterials, Cellular and Molecular Theranautics, Vellore Institute of Technology (VIT), Vellore, Tamil Nadu 632014, India

Abstract : Thrombosis, resulting from platelet adhesion and attachment is one of the major issues with blood contacting implants. Limiting platelet adhesion is highly desirable to ensure the usefulness of implants in blood contacting applications. In this work, we report on simplistic low-temperature high strain-rate processing to minimize the platelet adhesion on biomedical grade stainless steel. In addition, processing was also done at low rotational speed to study the effect of strain rate during processing. At high rotational speed, the processed steel resulted in single-phase ultra-fine grain structure along with significantly lower metal ion-release and better hemocompatibility. In addition, increased cellular viability with no significant morphological aberrations were observed in processed specimen in Human Wharton's jelly derived mesenchymal stem cells (HW-MSCs). Higher resistance for platelet adhesion for the processed steel is explained by favorable electronic characteristics of the metal-oxide and short-range polar interactions at the cell-substrate interface. Higher stability of the metal-oxide on processed steel contributed towards reducing the metal-ion release and ensure better hemocompatibility.

Keywords: *Biomaterials; Interfaces; Microstructure; Grain boundaries; Platelet*

INTRODUCTION

Stainless steel and titanium are amongst most widely used materials for bio-implant applications. This is mainly driven by their high strength, toughness, satisfactory corrosion and wear resistance as well as superior biocompatibility[1-3]. These materials also find applications in intravascular components such as blood pumps, pacemaker leads, heart valves and stents [4, 5]. However, one of the major issues with the use of these materials for blood contacting applications is the adsorption of blood constituents i.e. proteins and platelets on the implant surface [6-8]. The protein-implant interaction occur spontaneously as soon as blood contacts the implant surface followed by platelet attachment and blood coagulation. The consequence of adsorption of blood constituents on an implant involves severe complications such as thrombosis, vasculitis, and inflammation [7]. Limiting protein and platelet adhesion on an implant surface is highly desirable to ensure their usefulness for blood contacting applications.

The interaction of implant with blood components is a complex phenomenon and is primarily driven by its surface characteristics. Surface charge, wettability and surface topography significantly influence the protein, platelet adhesion and attachment. Negative surface charge and hydrophilicity are known to impede the platelet adhesion [8]. Various approaches including microstructural refinement [9, 10], tailoring the surface chemistry [11] and surface texturing [12, 13] have been reported to control the cellular response as well as diminish protein and platelet adhesion. The existing pattering techniques for crystalline metals, offer limited control over morphology and length-scale. In contrast, microstructural refinement approach is highly versatile in that context. Here, we demonstrate a versatile high strain-rate processing technique for limiting platelet adhesion on stainless steel surface through microstructure control. In addition, the processed stainless steel surface showed reduced metal ion-release and slightly better hemocompatibility. Improved thromboresistance properties of processed stainless-steel surface is explained based on favorable electronic characteristics of the metal-oxide and short-range polar interactions at the cell-substrate interface.

*Email: harpreet.arora@snu.edu.in, Phone: (+91)-8130625504

EXPERIMENTAL DETAILS

Biomedical grade stainless steel, SS316L, was used in the current study. The surface properties of stainless steel were tailored using low-temperature high strain-rate deformation process known as submerged friction stir processing. The details about the process are given elsewhere [14]. Processing was done at two different tool rotational speeds of 388 rpm (designated as 388-RS henceforth) and 1800 rpm (designated as 1800-RS henceforth). All samples were polished down to 3000 grit followed by electro-polishing in 10% oxalic acid solution. Electron back scatter diffraction (EBSD), performed using FEI Quanta 3D FEG, was used to reveal the grain size and phase distribution for all specimens. The semiconductor properties of the thin oxide layer formed on base SS316L and processed specimen was obtained using Mott-schottky analysis [15]. A standard three electrode electrochemical system (Gamry, Interface 1000E) was used along with the ringer solution as an electrolyte. For Mott-schottky analysis, AC signal of 10 mV amplitude at 1000 Hz frequency and a step potential of 50 mV is swept in the cathodic direction from 0.25V to -0.5V to measure the capacitance, C. Cell assay was performed using Human Wharton's jelly derived mesenchymal stem cells (HW-MSCs, Hi Media, India). A colorimetric assay (MTT, Thermo Fisher Scientific) was performed to evaluate the cytotoxicity of the as-received SS316L and processed specimens. In addition, the morphological aberrations were studied using fluorescence microscopy analysis after staining with DAPI, PI, and Phalloidin as described elsewhere [16]. Hemolysis assay was performed as described by Lale et. Al [17] while platelet isolation was performed as explained by Verhuel [18]. In addition, the fibrinogen adhesion of the specimens was determined by ELISA assay (enzyme-linked immunosorbent). The specific details of these assay were given elsewhere [14]. Inductively coupled plasma mass spectrometry (ICP-MS; Thermo fisher Scientific Inc., USA) was used to trace ion concentration of iron, chromium and nickel ions in the ringer solution. One-way analysis of variance method followed by a Student's t-test was used to compare the various means of the triplicate samples of individual experiments and to identify the statistical significance. All the statistical analysis has been done using the statistical tool GraphPad Prism 7.0 and $*p < 0.05$, $**p < 0.01$, $***p < 0.001$ were considered as statistically significant.

RESULTS

Microstructure

The grain size got significantly refined from 22 μm for the base steel to 0.6 μm and 0.9 μm for 388-RS and 1800-RS specimen. The detailed information regarding microstructure analysis and details is given elsewhere [19]. As shown by the EBSD analysis, the base steel has austenite structure while 1800-RS has nearly 8% martensite phase. The fraction of martensite phase is significantly high at nearly 45% for the 388-RS specimen.

Contact Angle

The contact angle of the base SS316L, 388-RS and 1800-RS specimens was found to be $60^\circ \pm 3^\circ$, $50^\circ \pm 9^\circ$, $46^\circ \pm 2^\circ$ respectively. Thus, both the processed samples show lower contact angle compared to the base steel. The decrease in contact angle with grain refinement has been shown previously as well [20]. Higher contact angle and large variation in the value for 388-RS specimen is likely due to high martensite fraction. This might be also due to the difference in the nature or percentage composition of oxide layer formed on the surface of the specimen [21, 22].

Mott Schottky Analysis

The electronic properties of the metal in a metal-electrolyte environment were determined using Mott Schottky (M-S) analysis, a capacitive measurement technique [15, 23].

This technique is used to study the interface reactions between the specimen surface and biological moieties. Here, all the specimen shows n-type semiconductor behavior with positive slope and the flat band potential of the same is calculated using the M-S equation [22, 24]. The curves obtained are shown in Figure 1 and the results comprising rest potential and flat band potential of all the tested specimens were tabulated in Table 1.

Tested Specimen	Open circuit potential Eocp (mV)	Flat band potential, Efb (mV)	Difference (mV)
SS316L	-250±5	-430±6	180
388-RS	-258±12	-432±9	174
1800-RS	-440±7	-298±4	-142

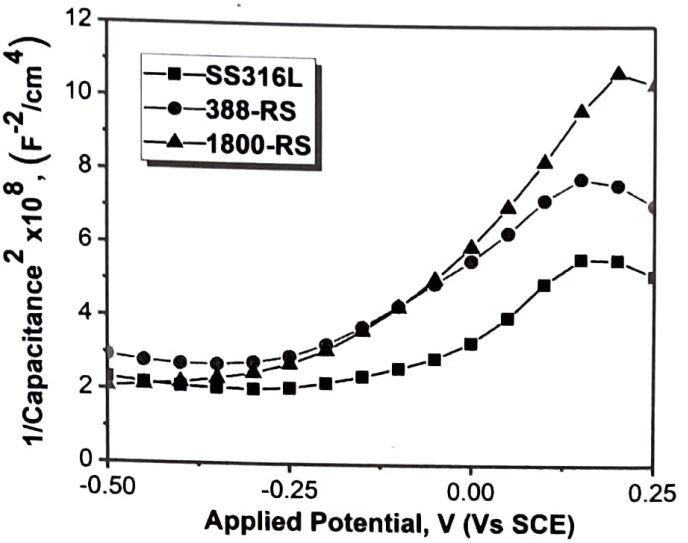

Fig.1: $1/C^2$ Vs E plot (Mott-Schottky) for stainless steel SS316L, low rotational speed friction processed SS316L (388-RS) and high rotational speed friction processed SS316L (1800-RS) at low temperature submerged conditions. Curves were obtained at 37° C in simulated body fluid environment (Ringer solution as electrolyte) using three-electrode electrochemical setup.

Table 1: Semi conducting properties of SS316L steel, low rotational speed friction processed SS316L (388-RS) and high rotational speed friction processed SS316L (1800-RS) at low temperature submerged conditions. Curves were obtained at 37°C in simulated body fluid environment (Ringer solution as electrolyte) using three-electrode electrochemical setup.

Interestingly, 1800-RS reported higher flat band potential and lower open circuit potential. Thus, the difference between the rest potential and flat band potential was calculated to be negative whereas other positive difference was observed in other specimens. Further, the consequences of this condition resulted in lesser platelet and fibrinogen adhesion on 1800-RS specimen which is discussed in forthcoming sections.

Hemocompatibility

The samples treated with human RBC reports minimal hemolysis for both the base SS316L and the processed samples (Figure 2(a)). Whereas total hemolysis was observed in the positive control (deionized water), < 5% hemolysis was detected for all the steel specimens. Although, all samples are hemocompatible, the percentage hemolysis is least for 1800-RS specimen.

Protein Adsorption and Platelet Adhesion

The adsorption of protein was determined by the adsorbed fibrinogen percentage which is shown in Figure 2(b). Here, polystyrene plate was used as the control. Both the processed specimen reported least fibrinogen adsorption compared to the base stainless-steel alloy with high statistical significance of $^{**}p < 0.05$. In addition, the release

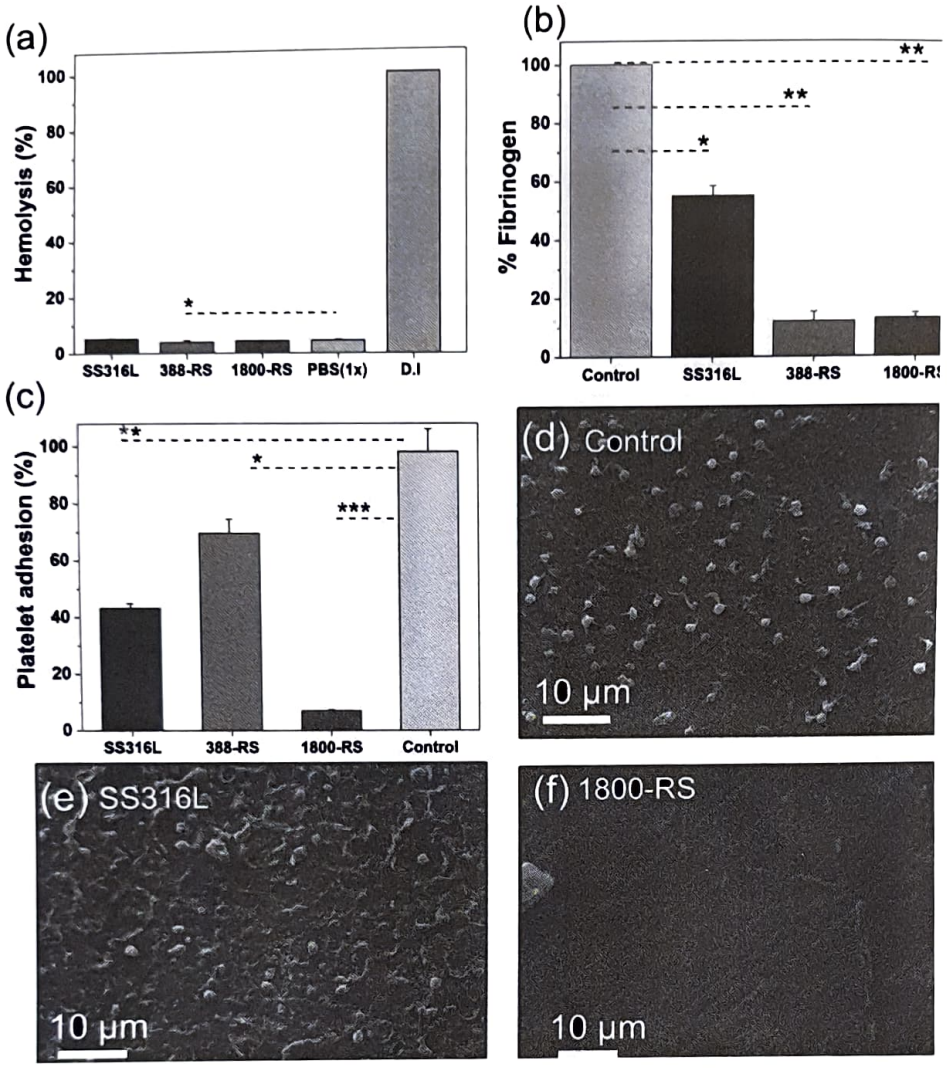

*Fig. 2: Hemocompatibility and platelet adhesion activity of the tested specimens: (a) hemolysis percentages, (b) % Fibrinogen adsorption obtained by ELISA, (c) % platelet adhesion obtained by LDH assay. Scanning electron microscopy (SEM) images of platelets adhering to (d) the control (polystyrene 24 well plate), (e) base stainless steel, SS316L and (f) high rotational speed friction processed SS316L (1800-RS). Data is presented along with error bar which represents standard deviation. *p < 0.05, **p < 0.01, ***p < 0.001 is considered to be statistically significant performed using student t-test.*

of lactate dehydrogenase (LDH) by the platelets on the samples was used to determine the platelet adhesion property and the results are shown in Figure 2(c). Platelets adhered on treated polystyrene plates were used as a control. 1800-RS specimen showed lowest platelet adhesion, nearly 7% compared to 43% for the base alloy. In contrast, 388-RS showed higher platelet adhesion of nearly 69%. Thus, the 1800-RS specimen exhibited exceptionally lower affinity for platelet adhesion, signifying its desirable attribute for blood-contacting implants. The statistical significance of $*p < 0.05$ in variation with respect to control is reported in all of the samples. However, higher statistical difference in 1800-RS was denoted using $***p < 0.001$. SEM images of control polystyrene plate, SS316L and the 1800-RS specimen, shown in Figure 2(d) and (e) and Figure 2(f) respectively, support minimal platelet adhesion on 1800-RS.

Cellular response - Cytotoxicity and Fluorescence microscopy Analysis

The results of cellular response of Human Wharton's jelly derived mesenchymal stem cells (HW-MSCs) is shown in Figure 3. Figure 3(a) shows the evaluated percentage of dead cells after MTT assay. It is seen that 1800-RS processed specimen shows less toxic nature compared to 388-RS and base SS316L alloy. In addition, the dead and live cells were stained using DAPI and PI respectively.

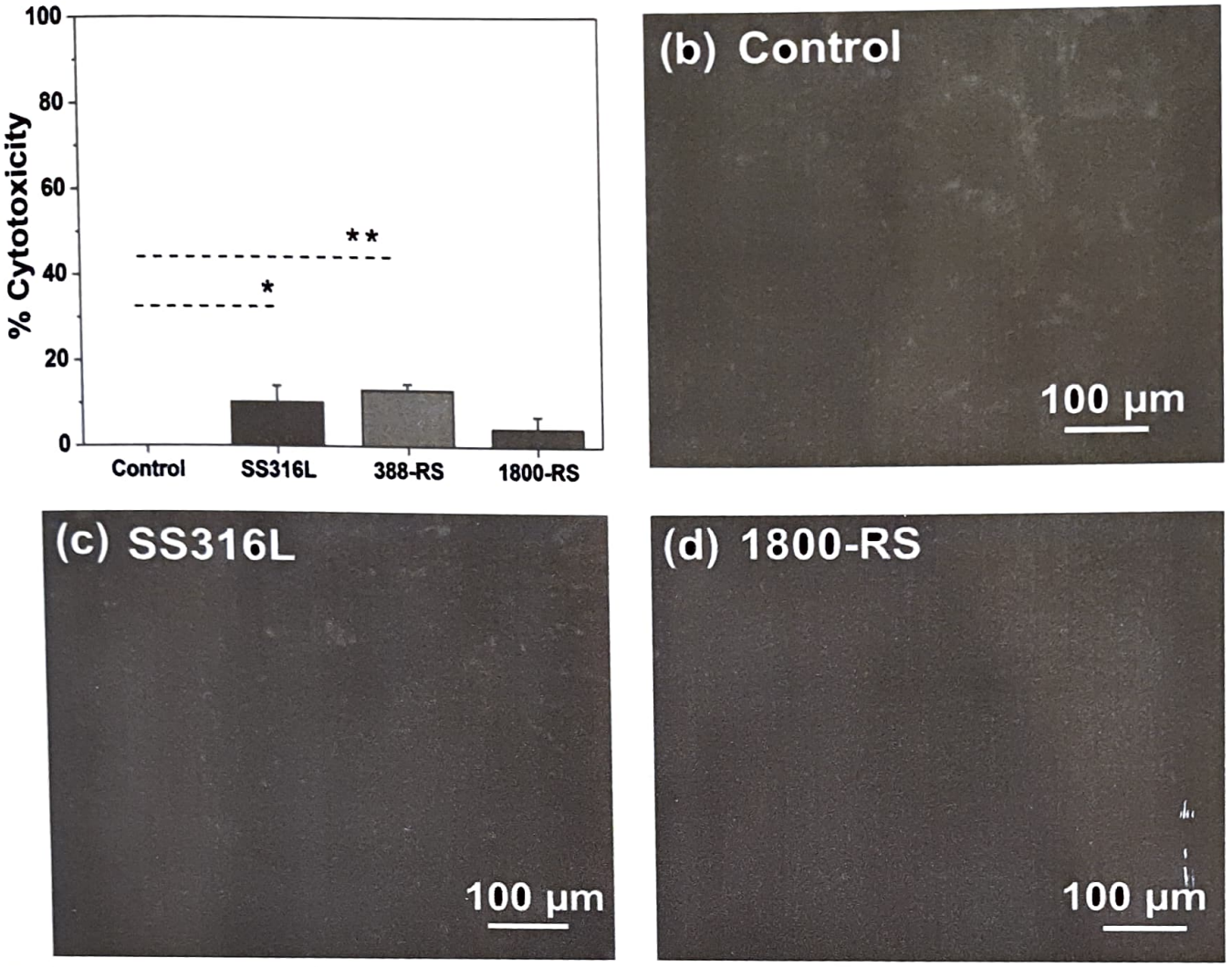

*Fig. 3: Cellular activity of the tested specimens: (a) % Toxicity obtained from MTT Assay, Fluorescence images of Human Wharton's jelly derived mesenchymal stem cells (HW-MSCs) cultured with respective conditioned media from the (b) control (media without specimen), (c) base SS316L alloy, (d) high rotational speed friction processed SS316L (1800-RS) for 48 h: Cells were stained DAPI , PI and phalloidin representing live cells (blue), dead cells (red) and actin filaments (green) respectively. Data is presented along with error bar which represents standard deviation. *p < 0.05, **p < 0.001 is considered to be statistically significant performed using student t-test.*

It is shown in Figure 3(b)-3(d) which indicates there is no significant difference in cell morphology after processing. Further, there was no red color fluorescence observed indicating processing does not affect the HW-MSCs morphology. Thus, providing safe condition as implant material for blood contacting applications.

ICP-MS Analysis

The results of ICP-MS testing for the base SS316L, 388-RS and 1800-RS specimens are given in Figure 4. Here, both the processed specimens released lesser ion compared to the base SS316L alloy.

In correlation with the weight percentage of the stainless steel, iron leached out the maximum compared to chromium and nickel. 1800-RS shows the lowest rate of ion release which corroborates the ability of 1800-RS to form a more stable passive layer in the ringer solution. These released ions from the implants results and inflammation [25, 26]. In addition, these elements can also lead to carcinogenic and mutagenic reactions [27, 28]. Thus, the reduction of leaching of ions using high rotational speed processing (1800-RS) from implant material might play a particular significance especially in blood contacting applications. in allergic reactions in the human body resulting in toxicity to the cells

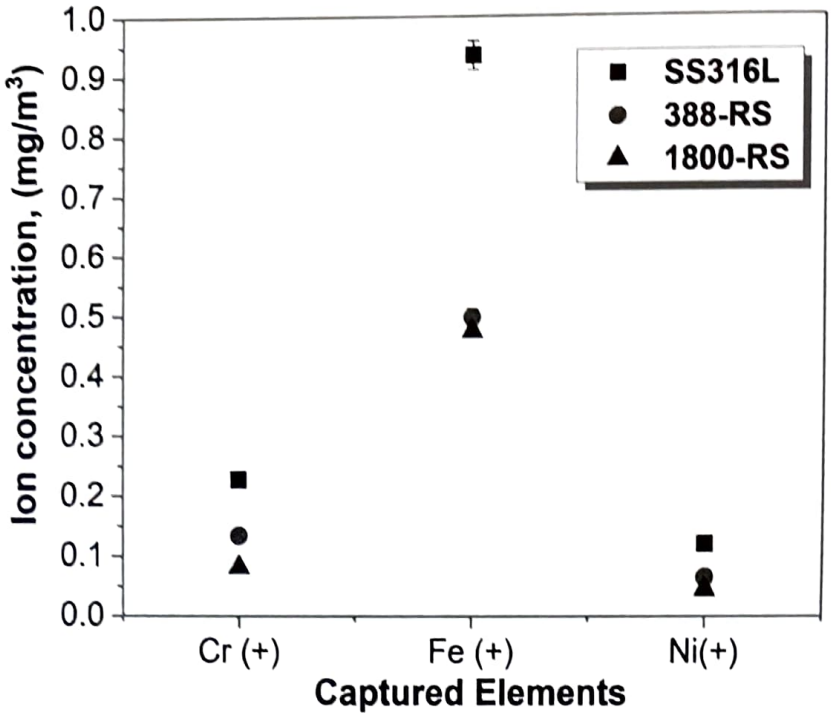

Fig. 4: Ion concentration of chromium, nickel and iron elements captured using Inductively coupled plasma mass spectrometry (ICP-MS) method for the base stainless steel SS316L, processed specimens at low rotational speed (388-RS) and high rotational speed (1800-RS) specimens that leach-out into the simulated body fluid environment. Both processed samples showed lower leaching of elements compared to the as-received alloy.

DISCUSSION

The results of the current study demonstrate that platelet adhesion was remarkably diminished in 1800-RS compared to the aggravated response for the base specimen. Platelet adhesion is a complex process & cannot be attributed to unique physico-chemical property. As per the extended DLVO (XDLVO) theory [29], the interaction of charged particle (such as platelets) with the substrate is a function of Lifshitz van der Waals, electrostatic double layer interaction and short-range polar interactions. While van der Waals energy is always positive, the electrostatic double layer interaction is attractive or repulsive depending on the substrate surface charge. Polar interactions become significantly important at short-range and basically govern the wettability state of the substrate. The platelet interactions with the substrate occur through a thin metal oxide layer that forms the outermost layer on the substrate. The nature of charge on the oxide layer plays an important role in platelet adhesion and attachment [8]. The Mott-Schottky analysis suggest lower rest potential for 1800-RS specimen compared to the flat band potential. The charge equilibrium necessitates transfer of excessive negative charge from the electrolyte to the oxide layer resulting in net negative surface charge for the 1800-RS specimen. The scenario is reversed for the base steel due to its higher rest potential than flat band, giving it a net positive charge. The short-range polar interactions which are nearly 10-100 times stronger than long-range interactions can play a more significant role [23, 30]. Both the processed samples are more hydrophilic compared to the base steel. The strong hydrogen bonding in hydrophilic surface presents a significant energy barrier for adhesion/bonding with other surfaces. Therefore, the decrease in platelet adhesion for 1800-RS specimen is likely explained by electrostatic repulsion between negatively charged substrate and the platelets as well as due to hydrophilic repulsion. In addition, processing does not affect the cellular morphology significantly. Further, the reduction in metal ion dissolution is likely attributed to more stable oxide layer on the processed specimen. Thus, the intervascular complications can be avoided by developing tailored microstructure using high strain-rate processing.

CONCLUSIONS

The microstructure of stainless steel got significantly refined by low temperature high strain-rate processing. Higher rotational speed processing resulted in nearly single-phase ultra-fine grain (UFG) structure while lower rotational speed processing resulted in dual-phase UFG structure. Single phase UFG steel showed significantly lower platelet adhesion, less toxicity and reduced metal-ion dissolution compared to base stainless steel. High resistance to platelet adhesion was attributed to negative surface charge induced by charge equilibrium at substrate-electrolyte interface and hydrophilic repulsion.

ACKNOWLEDGEMENTS

H.S. Arora thankfully acknowledge the financial assistance provided by Science and Engineering Research Board (SERB), Department of Science and Technology, under the project titled "Tailoring the Surface Properties of Crystalline and Amorphous Metals for Advanced Bio-Implants" (File no. YSS/2015/000678).

REFERENCES

[1] M. Sumita, S. Teoh, Durability of metallic implant materials, Engineering materials for biomedical applications, World Scientific 2-1-2-31, 2004.

[2] N. Eliaz, Degradation of implant materials, Springer Science & Business Media 2012.

[3] S.H. Teoh, Engineering materials for biomedical applications, World scientific 2004.

[4] M. Haidopoulos, S. Turgeon, C. Sarra-Bournet, G. Laroche, D. Mantovani, Development of an optimized electrochemical process for subsequent coating of 316 stainless steel for stent applications, Journal of Materials Science: Materials in Medicine 17(7): 647-657, 2006.

[5] G. Mani, M.D. Feldman, D. Patel, C.M. Agrawal, Coronary stents: a materials perspective, Biomaterials 28(9): 1689-1710, 2007.

[6] B. Thierry, Y. Merhi, L. Bilodeau, C. Trepanier, M. Tabrizian, Nitinol versus stainless steel stents: acute thrombogenicity study in an ex vivo porcine model, Biomaterials 23(14): 2997-3005, 2002.

[7] J. Courtney, N. Lamba, S. Sundaram, C. Forbes, Biomaterials for blood-contacting applications, Biomaterials 15(10): 737-744, 1994.

[8] V. DePalma, R. Baier, J. Ford, V. Gott, A. Furuse, Investigation of three-surface properties of several metals and their relation to blood compatibility, Journal of Biomedical Materials Research Part A 6(4): 37-75, 1972.

[9] E. Mostaed, M. Vedani, M. Hashempour, M. Bestetti, Influence of ECAP process on mechanical and corrosion properties of pure Mg and ZK60 magnesium alloy for biodegradable stent applications, Biomatter 4(1): e28283, 2014.

[10] C.S. Obayi, R. Tolouei, A. Mostavan, C. Paternoster, S. Turgeon, B.A. Okorie, D.O. Obikwelu, D. Mantovani, Effect of grain sizes on mechanical properties and biodegradation behavior of pure iron for cardiovascular stent application, Biomatter 6 (1): e959874, 2016.

[11] J. Eric Jones, M. Chen, Q. Yu, Corrosion resistance improvement for 316L stainless steel coronary artery stents by trimethylsilane plasma nanocoatings, Journal of Biomedical Materials Research Part B: Applied Biomaterials 102(7): 1363-1374, 2014.

[12] C. Hehrlein, M. Zimmermann, J. Metz, W. Ensinger, W. Kubler, Influence of surface texture and charge on the biocompatibility of endovascular stents, Coronary artery disease 6(7): 581-586, 1995.

[13] H. Zhao, J. Van Humbeeck, J. Sohier, I. De Scheerder, Electrochemical polishing of 316L stainless steel slotted tube coronary stents: an investigation of material removal and surface roughness, Progress in Biomedical Research 8: 70-81, 2003.

[14] G. Perumal, A. Ayyagari, A. Chakrabarti, D. Kannan, S. Pati, H.S. Grewal, S. Mukherjee, S. Singh, H.S. Arora, Friction Stir Processing of Stainless Steel for Ascertaining Its Superlative Performance in Bioimplant Applications, ACS applied materials & interfaces 9(42): 36615-36631, 2017.

[15] A. Di Paola, Semiconducting properties of passive films on stainless steels, Electrochimica Acta 34(2): 203-210, 1989.

[16] G. Perumal, H.S. Grewal, M. Pole, L.V.K. Reddy, S. Mukherjee, H. Singh, G. Manivasagam, H.S. Arora, Enhanced Biocorrosion Resistance and Cellular Response of a Dual-Phase High Entropy Alloy through Reduced Elemental Heterogeneity, ACS Applied Bio Materials 3(2): 1233-1244, 2020.

[17] S.V. Lale, A. Kumar, S. Prasad, A.C. Bharti, V. Koul, Folic acid and trastuzumab functionalized redox responsive polymersomes for intracellular doxorubicin delivery in breast cancer, Biomacromolecules 16(6): 1736-1752, 2015.

[18] H.M. Verheul, A.S. Jorna, K. Hoekman, H.J. Broxterman, M.F. Gebbink, H.M. Pinedo, Vascular endothelial growth factor–stimulated endothelial cells promote adhesion and activation of platelets, Blood 96(13): 4216-4221, 2000.

[19] G. Perumal, H. Grewal, H. Arora, Enhanced durability, bio-activity and corrosion resistance of stainless steel through severe surface deformation, Colloids and Surfaces B: Biointerfaces, 194: 111197, 2020.

[20] V. Muhonen, C. Fauveaux, G. Olivera, P. Vigneron, A. Danilov, M.D. Nagel, J. Tuukkanen, Fibronectin modulates osteoblast behavior on Nitinol, Journal of Biomedical Materials Research Part A, 88(3): 787-796, 2009.

[21] G. Perumal, H.S. Grewal, A. Ayyagari, S. Mukherjee, H.S. Arora, Enhancement in bio-corrosion resistance of metallic glass by severe surface deformation, Applied Surface Science 487: 1096-1103, 2019.

[22] S. Bahl, P. Shreyas, M. Trishul, S. Suwas, K. Chatterjee, Enhancing the mechanical and biological performance of a metallic biomaterial for orthopedic applications through changes in the surface oxide layer by nanocrystalline surface modification, Nanoscale 7(17): 7704-7716, 2015.

[23] G. Perumal, A. Chakrabarti, H.S. Grewal, S. Pati, S. Singh, H.S. Arora, Enhanced antibacterial properties and the cellular response of stainless steel through friction stir processing, Biofouling 35(2): 187-203,2019.

[24] N. Hakiki, S. Boudin, B. Rondot, M.D.C. Belo, The electronic structure of passive films formed on stainless steels, Corrosion Science 37(11): 1809-1822,1995.

[25] R.S. Nayak, B. Khanna, A. Pasha, K. Vinay, A. Narayan, K. Chaitra, Evaluation of nickel and chromium ion release during fixed orthodontic treatment using inductively coupled plasma-mass spectrometer: An in vivo study, Journal of International Oral Health: JIOH 7(8): 14,2015.

[26] E.K. Brooks, R.P. Brooks, M.T. Ehrensberger, Effects of simulated inflammation on the corrosion of 316L stainless steel, Materials Science and Engineering: C 71: 200-205, 2017.

[27] A. Lewis, J. Furze, S. Small, J. Robertson, B. Higgins, S. Taylor, D. Ricci, Long-erm stability of a coronary stent coating post-implantation, Journal of Biomedical Materials Research: An Official Journal of The Society for Biomaterials, The Japanese Society for Biomaterials, and The Australian Society for Biomaterials and the Korean Society for Biomaterials 63(6): 699-705, 2002.

[28] Y. Okazaki, E. Gotoh, Metal release from stainless steel, Co–Cr–Mo–Ni–Fe and Ni–Ti alloys in vascular implants, Corrosion Science 50(12: 3429-3438, 2008.

[29] C.J. van Oss, The extended DLVO theory, Interface Science and Technology, Elsevier, 31-48, 2008.

[30] C.J. Van Oss, M.K. Chaudhury, R.J. Good, Interfacial Lifshitz-van der Waals and polar interactions in macroscopic systems, Chemical Reviews 88(6): 927-941, 1988.